REFERENCES

[1] D. Cohen, "Simplified control of FFT hardware," *IEEE Trans. Acoust., Speech, Signal Processing*, vol. ASSP-24, pp. 577–579, Dec. 1976.

[2] L. G. Johnson, "Conflict free memory addressing for dedicated FFT hardware," *IEEE Trans. Circuits Syst. II*, vol. 39, pp. 312–316, May 1992.

[3] T. F. Ngai, M. J. Irwin, and S. Rawat, "Regular, area-time efficient carry lookahead adders," *J. Parallel Distrib. Comput.*, vol. 3, no. 1, pp. 92–105, Mar. 1986.

[4] M. C. Pease, "Organization of large scale fourier processors," *J. Assoc. Comput. Mach.*, vol. 16, pp. 474–482, July 1969.

[5] B. P. Sinha, J. Dattagupta, and A. Sen, "A cost effective FFT processor using memory segmentation," in *Proc. IEEE ISCAS*, 1983, vol. 1, pp. 20–23.

A Low-Power Phase-Splitting Adaptive Equalizer for High Bit-Rate Communication Systems

Rajamohana Hegde and Naresh R. Shanbhag

***Abstract*— A low-power architecture for a phase-splitting passband equalizer (PSPE) is proposed in this correspondence. The Hilbert relationship between the in-phase and quadrature-phase equalizers in the PSPE is exploited to develop the proposed architecture. It is shown via analysis and simulations that in a 51.84-Mb/s ATM-LAN environment, the proposed receiver results in 1) a net saving in power if the length of the Hilbert filter is less than 130, and 2) a saving of up to 20% can be achieved with a degradation in signal-to-noise ratio of less than 0.5 dB.**

***Index Terms*—ATM-LAN, CAP, Hilbert transform, low-power.**

I. INTRODUCTION

In recent years, the development of low-power devices for applications in fields of communications and DSP has become an active area of research due to the proliferation of mobile communication systems. It is for this reason that numerous power reduction techniques have been proposed starting at the algorithmic-level [1]–[4], architectural level [5], logic level [6], and the circuit level [1]. These techniques are currently being applied to develop low-power and high-speed transceivers for applications such as asymmetric digital subscriber loop (ADSL) [7], high-speed digital subscriber loop [8], and ATM-LAN [9] to achieve high bit rate digital communication over bandlimited channels.

The transceivers in most of these applications employ some form of adaptive equalization at the receiving end to combat corruption of the transmitted signal due to several sources of distortion such as intersymbol interference (ISI), crosstalk, and additive noise. In many of these applications, transmission schemes such as quadrature amplitude modulation (QAM) are employed, where the receiver consists of a phase splitter or a Hilbert transformer followed by a complex equalizer operating in either baseband or passband. In case of passband equalization, a simpler structure called the phase-splitting passband equalizer (PSPE) [10] can be employed, where the functions of phase splitter and equalizer are combined. The carrierless AM/PM (CAP) transmission scheme has been chosen by the Technical Committee of the ATM forum as the ATM-LAN physical layer interface standard at 51.84 Mb/s for category 3 unshielded-twisted-pair (UTP) wiring [9]. In CAP transceivers, a PSPE is employed at the receiving end. This receiver consists of a parallel arrangement of two adaptive equalizers. In this correspondence, we propose a low-power architecture for the PSPE employed in a CAP transceiver by exploiting the Hilbert relationship between the optimum solutions of the receive filters.

The rest of this correspondence is organized as follows. In the next section, we describe the generic CAP transceiver scheme. In Section III, we present the proposed receiver architecture and analyze its properties. In Section IV, we show, via analysis and simulation results, that the proposed architecture results in considerable saving in power in an ATM-LAN environment with marginal degradation in performance.

Manuscript received April 14, 1997; revised February 19, 1998. This work was supported by the National Science Foundation under CAREER Award MIP-9623737. The associate editor coordinating the review of this paper and approving it for publication was Dr. Elias Manolakos.

The authors are with the Coordinated Science Laboratory/Electrical and Computer Engineering Department, University of Illinois at Urbana-Champaign, Urbana, IL 61801 USA (e-mail: rhegde@uivlsi.csl.uiuc.edu; shanbhag@uivlsi.csl.uiuc.edu).

Publisher Item Identifier S 1053-587X(99)01359-8.

II. THE CAP TRANSMISSION SCHEME

The block diagram of the generic CAP transmitter is shown in Fig. 1(a). The bit stream to be transmitted is passed through a scrambler in order to randomize the data and are then fed into an encoder. The encoder maps a block of m bits into one of $k = 2^m$ unique complex symbols $S_n = r_n + jq_n$ in a k-CAP scheme. In the 16-CAP scheme described here, we have $m = 4$ and $k = 16$. The impulse responses of the shaping filters $p(kT')$ and $\tilde{p}(kT')$ are given by $p(kT') = g(kT')\cos 2\pi f_c kT'$ and $\tilde{p}(kT') = g(kT')\sin 2\pi f_c kT'$, where $g(kT') = g(t)|_{t=kT'}$ is the baseband pulse, and f_c is a frequency that is greater than the largest frequency component in $g(t)$. Note that the shaping filter impulse responses form a Hilbert pair [11], i.e.,

$$\tilde{p}(n) = h_I(n) * p(n), \text{ where } h_I(n) = \begin{cases} \dfrac{2\sin^2(\pi n/2)}{\pi n}, & n \neq 0 \\ 0, & n = 0. \end{cases} \tag{1}$$

Due to the Hilbert relationship, the magnitude response of $\tilde{p}(n)$ is the same as that of $p(n)$, but the phase response of $\tilde{p}(n)$ is shifted by $+90$ and -90° in the $+ve$ and $-ve$ frequency regions, respectively. The CAP receiver, which is shown in Fig. 1(b), consists of an analog-to-digital (A/D) converter operating at sampling frequency $1/T'$ followed by two adaptive digital filters in parallel [10], which are also operating at sampling frequency of $1/T' = K/T$, where K is the oversampling factor, and T is the symbol period. In the 16-CAP scheme, we have $K = 4$. These filters form the in-phase and quadrature-phase equalizers. The filter (**F**) block in these equalizers consist of an FIR filter whose coefficients are computed recursively in the weight up-date (WUD) block using the popular least mean squares (LMS) algorithm [12]. This algorithm minimizes the mean squared error (MSE) given by

$$\text{MSE} = \langle e_I(nT)^2 + e_Q(nT)^2 \rangle \tag{2}$$

where $\langle\,\rangle$ denotes expectation. The performance measure for the receiver in this equalization scheme is the signal-to-noise ratio (SNR) at the output (SNR_o) of the equalizer given by [13]

$$\text{SNR}_o = 10 \times \log_{10} \frac{\sigma_d^2}{\text{MSE}} \tag{3}$$

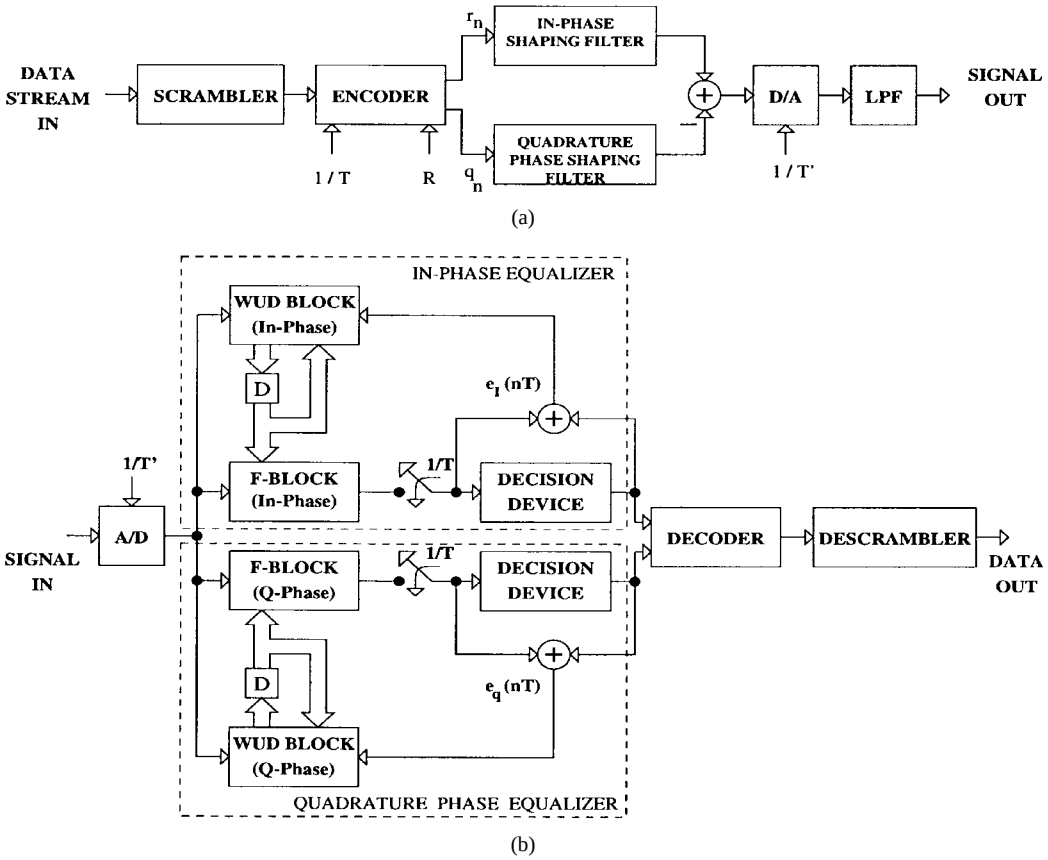

Fig. 1. CAP. (a) Transmitter. (b) Receiver.

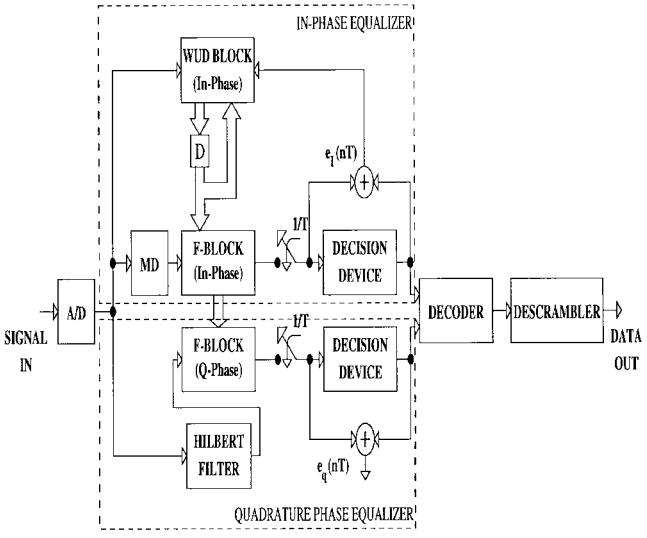

Fig. 2. Proposed low-power receiver.

where σ_d^2 is the variance of the desired signal. The outputs of the equalizers are sampled at the symbol rate $(1/T)$ and fed to a decision device followed by a decoder. Additional details regarding the generic CAP scheme, the 16-CAP transmitter, and CAP receiver can be found in [9].

III. The Proposed Receiver Structure

In this section, we show how the Hilbert relationship between the in-phase and quadrature-phase equalizers of the CAP receiver can be exploited to obtain the proposed structure. We then compute the power consumed by the CAP equalizer and the proposed equalizer

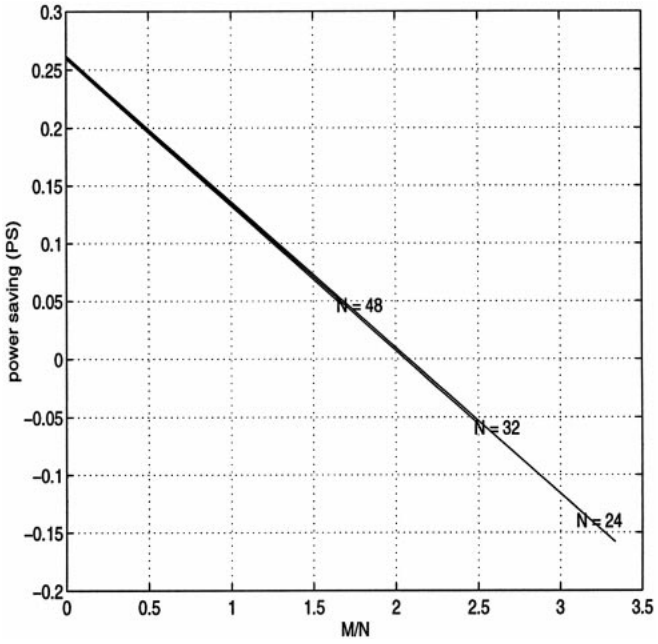

Fig. 3. Plot of percentage of power saved versus M/N.

and show that the proposed equalizer can lead to a substantial amount of power savings with marginal degradation in performance.

A. CAP Equalizer

As mentioned before, the shaping filter impulse responses in a CAP transceiver form a Hilbert pair. In [13], it has been shown that the optimum minimum mean squared error (MMSE) solutions for

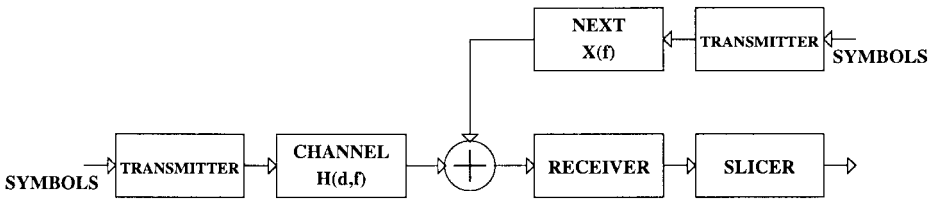

Fig. 4. Simulation setup for the CAP system.

these equalizers also form a Hilbert pair. If the in-phase and the quadrature receive filter impulse responses are denoted by $f(n)$ and $\tilde{f}(n)$, respectively, then $\tilde{f}(n) = h_I(n) * f(n)$, where the symbol $*$ denotes convolution. Let $y_i(n)$ and $y_q(n)$ denote the in-phase and the quadrature components of the receive filter output, respectively, and let $x(n)$ denote the input. The equalizer outputs can be expressed as

$$\begin{aligned} y_i(n) &= f(n) * x(n) \\ y_q(n) &= \tilde{f}(n) * x(n) = f(n) * [h_I(n) * x(n)]. \end{aligned} \tag{4}$$

From (4), we see that $y_q(n)$ can be computed as the output of the in-phase filter with the Hilbert transform of $x(n)$ as the input. Hence, the CAP receiver can be modified as shown in Fig. 2. The proposed structure in Fig. 2 is functionally identical to the original CAP receiver shown in Fig. 1(b) as long as the Hilbert transformer is of infinite length. In practice, we employ a finite-length Hilbert transformer given by

$$h_F(n) = \begin{cases} h_I(n), & \text{for } -M \le n \le M \\ 0, & \text{elsewhere.} \end{cases} \tag{5}$$

The performance of a receiver with a finite-length Hilbert transformer will be degraded as compared with the original CAP receiver. In Section III-C, we derive an analytical expression to estimate this degradation, given the length of the Hilbert transformer.

The proposed receiver structure shown in Fig. 2 has several attractive features.

1) The WUD block in the quadrature filter is completely eliminated.
2) The quadrature filter can be pipelined with little additional hardware overhead due to the elimination of feedback.
3) In a blind start-up scheme, as there is only one adaptive equalizer, the possible erroneous solutions are fewer for the proposed structure.

However, there is the addition of the Hilbert filter in the feedforward path of the quadrature arm. Hence, the proposed structure would result in power savings as long as the complexity of the Hilbert filter is smaller than that of the WUD block. The tradeoff between power savings and performance is explored in the next two subsections.

B. Power Savings

In this subsection, we compute the power savings achieved via the proposed equalizer by first computing the power dissipation of the traditional CAP receiver [see Fig. 1(b)] and then comparing it with that of the proposed structure (see Fig. 2). The traditional CAP receiver [see Fig. 1(b)] has two adaptive filters of length N. Each adaptive filter consists of N taps, each containing two multipliers (one in the **F** block and one in the WUD block); one single precision adder (in the **F** block); and one double precision adder (in the WUD block). In addition to this, the **F** block consists of a single precision adder to compute the error across the slicer, and the WUD block consists of a multiplier to compute the term $\mu X(n)$ in the LMS algorithm [12]. Let the average switching capacitance of a single precision adder be denoted by C_a. The average power dissipated by this adder [1] is then given by $P_a = C_a V_{dd}^2 f$, where V_{dd} is the supply voltage, and f is the average switching frequency. Assuming that the switching capacitances of the multiplier and double precision adders are $K_m C_a$ and $K_a C_a$, the average power dissipated by a CAP receiver of length N (P_{CAP}) is given by

$$P_{\mathrm{CAP}} = 2[(2N+1)K_m + NK_a + (N+1)]C_a V_{dd}^2 f. \tag{6}$$

The proposed structure (see Fig. 2) consists of two **F** blocks, one WUD block, and a Hilbert transformer of length $2M+1$. The complexity requirements of the Hilbert filter ($M/2$ taps, each with one multiplier and two single precision adders, for M even) can be derived from the fact that the impulse response of the Hilbert filter in (1) and (5) is antisymmetric and is zero for even values of n. Hence, the average power dissipated by the proposed structure (P_{HIL}) is given by

$$P_{HIL} = \left[\left(3N + \frac{M}{2} + 1\right)K_m + NK_a + (2N + M + 1)\right] f C_a V_{dd}^2. \tag{7}$$

We can now obtain the expression for savings in power defined as $PS = (P_{\mathrm{CAP}} - P_{HIL})/P_{\mathrm{CAP}}$ as

$$PS = \frac{\left(1 - \frac{M}{2N} + \frac{1}{N}\right)K_m + K_a - \frac{M-1}{N}}{2\left[\left(2 + \frac{1}{N}\right)K_m + \left(1 + \frac{1}{N}\right)K_a + 1\right]}. \tag{8}$$

In order to have $PS > 0$, we need to choose M and N such that

$$\frac{M}{N} < \frac{\left(1 + \frac{1}{N}\right)K_m + K_a + \frac{1}{N}}{1 + \frac{K_m}{2}}. \tag{9}$$

Fig. 3 shows the plot of the *%savings* in power versus the ratio of M/N for $N = 24$, 32 and 48, $K_m = 16$, and $K_a = 2$. Note that the three curves are nearly identical and that there is a net saving in power as long as the length of the Hilbert filter is less than 130 for $N = 32$.

C. Excess MSE

We now derive an expression to compute the decrease in SNR_o due to the use of finite-length Hilbert filter. Note that the maximum value of SNR_o achievable via the proposed structure (see Fig. 2) with an infinite length Hilbert filter is the same as that achieved by the original CAP structure [see Fig. 1(b)].

The output of the quadrature-phase filter in the proposed receiver $y_q(n)$ is given by $y_q(n) = \sum_{k=0}^{N-1} w_{opt}(k)\tilde{x}(n-k)$, where $\tilde{x}(n) = \sum_{k=-M}^{M} h_F(k)x(n-k)$. If the Hilbert filter were of infinite length, the output of the quadrature filter would be $y_q'(n) = \sum_{k=0}^{N-1} w_{opt}(k)\tilde{x}'(n-k)$, where $\tilde{x}'(n) = \sum_{k=-\infty}^{\infty} h_I(k)x(n-k)$. Let $b(n) = q(n-\Delta)$ denote the quadrature component of the desired sequence, where Δ is the overall delay from the transmitter to the receiver. Let $e_Q(n)$ and $e_Q'(n)$ denote the quadrature error sequence when the Hilbert filter is of finite length and infinite length,

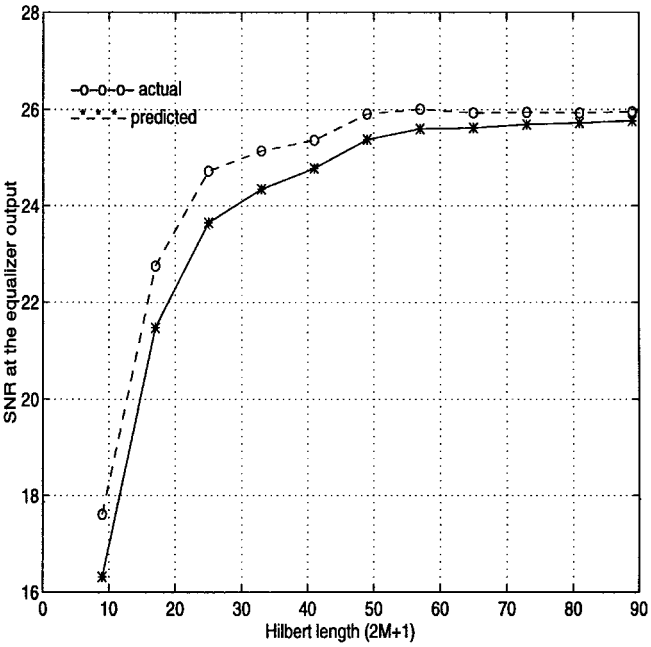

Fig. 5. Plot of SNR_o versus Hilbert filter length $(2M+1)$.

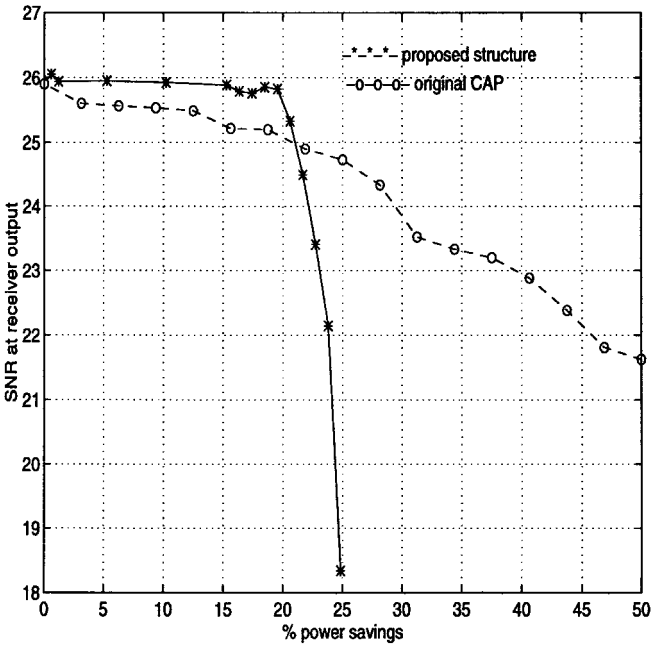

Fig. 6. Plot of SNR_o versus power savings (ps).

respectively. We then obtain the excess error $e_{EX}(n)$ due to the use of a finite length Hilbert filter as

$$e_{EX}(n) = e_Q(n) - e'_Q(n) = \sum_{k=0}^{N-1} w_{opt}(k)\left[\sum_{k=-\infty}^{\infty} h_{err}(k)x(n-k)\right] = \mathbf{W}_{opt}^T \mathbf{X}_{err} \quad (10)$$

where $e'_Q(n) = b(n) - y'_q(n)$, $e_Q(n) = b(n) - y_q(n)$

$$h_{err}(n) = \begin{cases} h_I(n), & n \le -M \text{ and } n \ge M \\ 0, & \text{elsewhere.} \end{cases} \quad (11)$$

$\mathbf{W}_{opt}$ is the vector of optimum weights of the in-phase equalizer of length N, and $\mathbf{X}_{err}^T = [x_{err}(n) \quad x_{err}(n-1) \quad \cdots \quad x_{err}(n-N+1)]$ with $x_{err}(k) = \sum_{k=-\infty}^{\infty} h_{err}(k)x(n-k)$. Squaring both sides of (10) and taking expectation, we obtain

$$\langle e_{EX}^2 \rangle = \mathbf{W}_{opt}^T \mathbf{R}_{XX} \mathbf{W}_{opt} \quad (12)$$

where $\mathbf{R}_{XX} = \langle \mathbf{X}_{err} \mathbf{X}_{err}^T \rangle$. Given the channel model, both $\mathbf{R}_{XX}$ and the optimum weight vector $\mathbf{W}_{opt}$ can be easily computed. Note that $\mathbf{R}_{XX}$ is a function of $h_{err}(n)$, which in turn depends on the length of the Hilbert filter. Hence, we can employ (12) to estimate the increase in the MSE due to the finite-length Hilbert filter of length $(2M+1)$. In Section IV, we will verify (12) via comparison with simulation results.

IV. Simulation Results

In this section, the performance of the proposed structure functioning as a receive equalizer in an ATM-LAN transceiver, operating at 51.84 Mb/s over unshielded twisted pair (UTP-3) wiring, is evaluated. The block diagram of the system that was simulated is shown in Fig. 4. The two major causes of performance degradation for transceivers operating over UTP wiring employed in most ATM-LAN environments are propagation loss and near end crosstalk (NEXT) generated between pairs of wires in the same cable. In the experimental setup discussed in this section, the ATM channel is assumed to be a 100-m UTP-3 wire, and a "TIA/EIA" NEXT model [9] is employed.

The transceiver parameters chosen are [9] as follows:

- Bits per symbol: $m = 4$;
- Symbol rate: $1/T$ = 12.96 Mbaud;
- Excess bandwidth: $\alpha = 1$ (100%);
- Center frequency: $f_c = 12.96$ MHz;
- Bandwidth utilization: 25.92 MHz;
- Transmit shaping filter tap span: $4\ T$;
- Receive filter tap span: $8\ T$;
- Bit-error rate (BER) desired: 10^{-10}.

A desired BER of 10^{-10} translates to a desired SNR_0 of 23.25 dB at the output of the equalizer [9]. The original CAP receiver [see Fig. 1(b)] provided an SNR_o of 25.9 dB, which will be employed as a benchmark against which the performance of the proposed structure will be compared.

Experiment 1: The proposed receiver structure (see Fig. 2) is now employed in the same channel, and its performance is evaluated when Hilbert transformers of several lengths are employed. The spans of the in-phase adaptive filter and the quadrature-phase FIR filter are fixed at $8\ T$. The length of the Hilbert filter is varied, and the SNR_o values are compared against those predicted using the expression for the *excess error* derived in (12). The results shown in Fig. 5 indicate that the analysis and simulations match quite well. For very low values of the Hilbert filter lengths, the SNR_o values are lower than the desired threshold. However, we obtain SNR_o values of more than 25 dB, when the Hilbert transformer length is more than 33. This value asymptotically approaches 25.9 dB as the Hilbert transformer length increases. Per our analysis of power consumption in Section III-B, a net power saving is obtained as long as the length of the Hilbert filter is less than 130. Therefore, the proposed structure will provide a noise margin better than 1.75 dB and enable power saving as long as the Hilbert transformer length is greater than 33 and less than 130. For example, when the Hilbert filter lengths are 33 and 41, the SNR_o values are 24.6 and 25.412 dB, and the corresponding power saving is more than 20 and 18%, respectively.

Experiment 2: Power reduction with some tradeoff in SNR_0 can also be obtained by employing the traditional CAP equalizer in Fig. 1(b) with reduced number of taps. In this subsection, the power

reduction and the resulting degradation in SNR_o obtained by employing a reduced length traditional equalizer is studied. The values of SNR_o for the traditional receiver with tap lengths varying from 16 to 32 were obtained, and these values are plotted against the corresponding power saving (dotted line) in Fig. 6. The figure also shows the corresponding plot for the proposed structure. The following conclusions can be drawn from Fig. 6: 1) If the desired SNR_o is more than 25.0 dB, the proposed structure offers higher power savings than the original structure even if the number of taps is reduced; 2) for lower values of desired SNR_o, the original structure with lesser taps saves more power. However, if the desired BER is lower than 10^{-10}, the original structure would then need a higher number of taps, and in that case, the proposed structure in Fig. 2 would lead to higher power savings as compared with the original structure in Fig. 1(b).

We also compared the performance of the proposed structure to that of the original structure in presence of phase offset at the input. The degradation in performance due to phase offset of 4, 8, and 12 sample delays was measured for both the original structure and the proposed structure with Hilbert filter length of 57. As expected, we observed that the degradation in performance in both cases is almost similar as a phase offset at the input does not alter the Hilbert relationship between the I- and the Q-phase equalizers. However, for general channel nonidealities, the degradation in performance for the proposed structure could be higher as the quadrature-phase equalizer is not adapted independently.

V. Conclusions

In this correspondence, we have presented a low-power architecture for the PSPE by exploiting the Hilbert relationship between the in-phase and quadrature-phase equalizers. Future extensions could include consideration of low-complexity LMS and Hilbert filter structures and applications to other broadband systems such as a very-high-speed digital subscriber loop (VDSL).

References

[1] A. Chandrakasan and R. W. Brodersen, "Minimizing power consumption in CMOS digital circuits," *Proc. IEEE,* vol. 83, pp. 498–523, Apr. 1995.

[2] E. Tsern and T. H. Meng, "A low power video rate pyramid VQ decoder," *IEEE J. Solid-State Circuits,* vol. 31, pp. 1789–1794, Nov. 1996.

[3] K. K. Parhi, "Algorithm transformation techniques for concurrent processors," *Proc. IEEE,* vol. 77, pp. 1879–1895, Dec. 1989.

[4] N. R. Shanbhag and K. K. Parhi, *Pipelined Adaptive Digital Filters.* Boston, MA: Kluwer, 1994.

[5] M. Potkonjak and J. Rabaey, "Fast implementation of recursive programs using transformations," in *Proc. ICASSP,* San Francisco, CA, Mar. 1992, pp. V.569–V.572.

[6] M. Alidina *et al.,* "Precomputation based sequential logic optimization for low-power," *IEEE Trans. VLSI Syst.,* vol. 2, pp. 426–436, Dec. 1994.

[7] P. S Chow, J. C. Tu, and J. M. Cioffi, "Performance evaluation of a multichannel transceiver system for ADSL and VHDSL services," *IEEE J. Select. Areas Commun.,* vol. 9, pp. 900–919, Aug. 1991.

[8] D. W. Lin, C.-T. Chen, and T. R. Hsing, "Video on phone lines: Technology and applications," *Proc. IEEE,* vol. 83, pp. 175–193, Feb. 1995.

[9] G.-H. Im and J. J. Werner, "51.84 Mb/s 16-CAP ATM-LAN standard," *IEEE J. Select. Areas Commun.,* vol. 13, pp. 620–632, May 1995.

[10] F. Ling and S. U. H. Qureshi, "Convergence and steady-state behavior of a phase splitting fractionally spaced equalizer," *IEEE Trans. Commun.,* vol. 38, pp. 418–425, Apr. 1990.

[11] E. A. Lee and D. G. Messerschmitt, *Digital Communication.* Boston, MA, Kluwer, 1994.

[12] S. Haykin, *Adaptive Filter Theory.* Englewood Cliffs, NJ: Prentice-Hall, 1991.

[13] W. Y. Chen, G-H. Im, and J. J. Werner, "Design of digital carrierless AM/PM transceivers," AT&T/Bellcore Contribution T1E1.4/92-149, Aug. 19, 1992.